

Full-State Tracking and Internal Dynamics of Nonholonomic Wheeled Mobile Robots

Danwei Wang and Guangyan Xu

Abstract—In this paper, the stable full-state tracking problem is investigated for nonholonomic wheeled mobile robots under output-tracking control laws. Dynamics of such wheeled mobile robots are nonholonomic and pose challenging problems for control design and stability analysis. The dynamics formulated in terms of full-state tracking errors offer some properties that allow better understanding of the internal and zero dynamics of the tracking-error system and more insights to the trajectory tracking stability. Output functions are chosen as virtual reference points for various types of wheeled mobile robots in aid of output controller designs. Sufficient conditions are derived to ensure the stable full-state trajectory tracking under output-tracking control laws. A type (1, 1) mobile robot of car-like configuration is studied in detail and further numerical analysis provides more results which are beyond the reach of analytical means. An example and simulation results are presented to confirm the theory and observations.

Index Terms—Nonholonomic dynamics, tracking stability, wheeled mobile robots, zero dynamics.

I. INTRODUCTION

IN THE last decade, feedback control for wheeled mobile robots has been extensively studied. There are two main control tasks for nonholonomic wheeled mobile robots, i.e., stabilizing to an equilibrium point (such as parking) and stabilizing to an equilibrium manifold (such as trajectory tracking or path following). The first control task is considered challenging because a nonholonomic system cannot be stabilized to an equilibrium point by a smooth state feedback [1], [2]. To overcome these difficulties, substantial efforts have been spent to develop sophisticated state-feedback-control laws, such as nonsmooth feedback laws [3], [4], time-varying feedback laws [5], [6], and middle (nonsmooth and time-varying) feedback laws [7], [8]. The second problem is the stabilization to an equilibrium manifold and is not subject to the difficulties as in the previous case. Because the outputs that have the same dimension as the inputs can be defined, classical nonlinear control theories can be used to solve the output-tracking problem of nonholonomic systems [9]–[13]. Furthermore, the (static or dynamic) input–output feedback linearization technique is well studied and proved to be effective for output-tracking control.

In mobile robot-motion control, output-trajectory tracking is insufficient in most situations. Full-state tracking is required to ensure smooth and successful maneuvers. Some works are de-

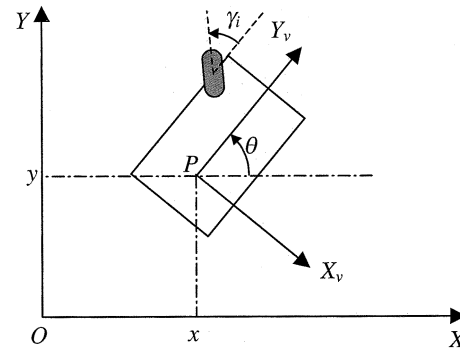


Fig. 1. Mobile robot with steerable wheels.

voted to this problem such as control designs by the Lyapunov direct method [14], approximate linearization [15], and recursive backstepping [16]. Static input–output feedback-linearization techniques have been widely used for wheeled mobile systems [9], [18]. These works successfully transform closed-loop input–output into linear dynamics, and then, control designs become a straightforward task. However, such nonholonomic dynamics possess nonlinear internal dynamics. The stability of the internal dynamics is critical for a feedback control law to work properly. So far, few efforts were spent to analyze this internal dynamic behavior. One interesting observation was made on the stability of internal dynamics in [17]. The study was on the internal stability of a two-wheel differentially steered mobile robot. Internal dynamics exhibit unstable properties when the mobile robot tracks a trajectory that moves backward.

In this paper, we study the full-state tracking-stability issues in the mobile robots with restricted mobility. We also investigate the relationship between the full-state tracking stability and internal and zero dynamics for general configurations of nonholonomic wheeled mobile robots. The analysis is carried out in the tracking-error dynamics that offer useful properties and insights. An approach is developed using linear approximation and sufficient conditions are provided for full-state tracking stability. A special car-like mobile robot is studied in detail to enhance and visualize the results. Numerical analysis is also deployed to obtain some interesting observations. An example and simulation results are also presented to illustrate the developed theory.

II. DYNAMICS AND FORMULATION

We consider wheeled mobile robots moving on a horizontal plane, as shown in Fig. 1. The wheeled mobile robots are classified according to the mobility $1 \leq m \leq 3$ and the

Manuscript received August 1, 2002; revised January 20, 2003. Recommended by Guest Editors C. Mavroidis, E. Papadopoulos, and N. Sarkar.

The authors are with the School of Electrical and Electronic Engineering, Nanyang Technological University, Singapore 639798 (e-mail: edwwang@ntu.edu.sg).

Digital Object Identifier 10.1109/TMECH.2003.812832

TABLE I
MATRIX $Q(\gamma)$ AND VECTOR $b^T(\gamma)$ FOR NONHOLONOMIC WHEELED
MOBILE ROBOT

Type (m, s)	Type (2,0)	Type (2,1)	Type (1,1)	Type (1,2)
$Q(\gamma) \in R^{2 \times m}$	$\frac{1}{2} \begin{bmatrix} 1 & 1 \\ 0 & 0 \end{bmatrix}$	$\begin{bmatrix} \cos \gamma_1 & 0 \\ \sin \gamma_1 & 0 \end{bmatrix}$	$\begin{bmatrix} 1 \\ 0 \end{bmatrix}$	$\begin{bmatrix} \cos \gamma_1 \cos \gamma_2 \\ \frac{1}{2} \sin(\gamma_1 + \gamma_2) \end{bmatrix}$
$b^T(\gamma) \in R^m$	$[-\frac{1}{a} \quad \frac{1}{a}]$	$[0 \quad 1]$	$\frac{1}{a} \tan \gamma_1$	$\frac{1}{a} \sin(\gamma_1 - \gamma_2)$

★ Parameter a in the table is the wheel-thread [type (2, 0) robot] or wheel-base [type (1, 1) and type (1, 2) robot].

steerability $0 \leq s \leq 2$ as type (m, s) mobile robot [11]. If the wheeled mobile robot is equipped with fixed and/or steering wheels, the mobility of robot is restricted ($m \leq 2$) and the system is nonholonomic. Suppose that there is no skidding between the wheels and the ground. The dynamics of these mobile robots can be described by the following differential equations (an extension from [11]):

$$\dot{\zeta} = R^T(\theta)Q(\gamma)v \quad (1)$$

$$\dot{\theta} = b^T(\gamma)v \quad (2)$$

$$\dot{\gamma} = \omega \quad (3)$$

$$\dot{v} = u_m \quad (4)$$

$$\dot{\omega} = u_s \quad (5)$$

where the vector $\zeta = [x \ y]^T$ represents the coordinates of a reference point P on the robot in the inertial frame XOY , and θ is the heading angle as defined in Fig. 1. The s -vector $\gamma = [\gamma_1, \dots, \gamma_s]^T$ represents the steering coordinates of independent steering wheels. Both vectors $v \in R^m$ and $\omega \in R^s$ are homogeneous to velocities. Both vectors $u_m \in R^m$ and $u_s \in R^s$ are control inputs homogeneous to torques. In (1), the matrix $R(\theta)$ is a rotation matrix given as follows:

$$R(\theta) = \begin{bmatrix} \cos \theta & \sin \theta \\ -\sin \theta & \cos \theta \end{bmatrix}. \quad (6)$$

The matrix $Q(\gamma) \in R^{2 \times m}$ and vector $b(\gamma) \in R^m$ in (1) for each type of nonholonomic wheeled mobile robots are listed in Table I.

Equations (1)–(5) can be rewritten as follows:

$$\dot{q} = G(\theta, \gamma)\mu \quad (7)$$

$$\dot{\mu} = u \quad (8)$$

where

$$q = \begin{bmatrix} \zeta \\ \theta \\ \gamma \end{bmatrix} \quad \mu = \begin{bmatrix} v \\ \omega \end{bmatrix} \quad u = \begin{bmatrix} u_m \\ u_s \end{bmatrix}$$

$$G(\theta, \gamma) = \begin{bmatrix} R^T(\theta)Q(\gamma) & 0 \\ b^T(\gamma) & 0 \\ 0 & I_s \end{bmatrix}.$$

TABLE II
OUTPUT FUNCTIONS AND REGULAR CONDITIONS

Type (m, s)	Type (2,0)	Type (2,1)	Type (1,1)	Type (1,2)
$\gamma^1 \in R^{m+s-2}$	null	γ_1	null	γ_2
$\gamma^2 \in R^{2-m}$	null	null	γ_1	γ_1
$d(\gamma^2) \in R^2$	$\begin{bmatrix} l \\ 0 \end{bmatrix}$	$\begin{bmatrix} l \cos \gamma_1 \\ l \sin \gamma_1 \end{bmatrix}$	$\begin{bmatrix} a + l \cos(p\gamma_1) \\ l \sin(p\gamma_1) \end{bmatrix}$	$\begin{bmatrix} \frac{a}{2} + l \cos \gamma_1 \\ l \sin \gamma_1 \end{bmatrix}$
Regular conditions	$l \neq 0$	$l \neq 0$ $ \gamma_1 < \frac{\pi}{2}$	$lp \neq 0$ $ 1-p < \frac{\pi}{2\gamma_{1max}}$ $ \gamma_1 < \gamma_{1max} < \frac{\pi}{2}$	$l \neq 0$ $ \gamma_2 < \frac{\pi}{2}$

For the mobile robot with restricted mobility, the steering coordinate vector γ can be further partitioned as follows:

$$\gamma = \begin{bmatrix} \gamma^1 \\ \gamma^2 \end{bmatrix} \quad (9)$$

with $\gamma^1 \in R^{m+s-2}$ and $\gamma^2 \in R^{2-m}$. It is easy to check that inequalities $0 \leq m+s-2 \leq 1$ and $0 \leq 2-m \leq 1$ must be valid and, consequently, both γ^1 and γ^2 are either a scalar or a null.

A property of nonholonomic system (7) and (8) is that the number of inputs in u is less than the number of generalized states in q , whose entries ($x, y, \theta, \gamma^1, \gamma^2$) are independent of each other. To facilitate the control design, most control theories, such as feedback linearization [9], [18] and robust control techniques [10], [12], and [13] require defining a set of output variable $z \in R^{m+s}$ which has the same dimension as the control input, i.e.,

$$z = h(q) \quad (10)$$

where, the output function $h(q): R^{3+s} \rightarrow R^{m+s}$ is an epimorphism. It is clear that different definitions of output functions leads to different control designs. Basically, the output (10) should be well defined to achieve decoupling between input–output dynamics and internal dynamics. As for the static-state feedback-control scheme [17], the following so-called decoupling matrix must be nonsingular:

$$E(\theta, \gamma) = \frac{\partial h(q)}{\partial q} \cdot G(\theta, \gamma). \quad (11)$$

To solve the tracking-control problem of mobile systems (7) and (8) by means of static-state feedback, the following output is defined:

$$h(q) = \begin{bmatrix} \zeta + R^T(\theta)d(\gamma^2) \\ \gamma^1 \end{bmatrix} \quad (12)$$

where, vector $\gamma^1 \in R^{m+s-2}$, $\gamma^2 \in R^{2-m}$, and $d(\gamma^2) \in R^2$ for each type of robot are given by Table II.

It is easy to check that the decoupling matrix of output function (12) is nonsingular if the regular conditions in Table II are satisfied. Furthermore, the $(m+s) \times (m+s)$ matrix $E(\theta, \gamma)$ can be decomposed into a product of two matrices as follows:

$$E(\theta, \gamma) = \begin{bmatrix} R^T(\theta) & 0 \\ 0 & I_{m+s-2} \end{bmatrix} \bar{E}(\gamma) \quad (13)$$

with

$$\bar{E}(\gamma) = \begin{bmatrix} Q(\gamma) + \begin{bmatrix} 0 & -1 \\ 1 & 0 \end{bmatrix} d(\gamma^2) b^T(\gamma) & \frac{\partial d(\gamma^2)}{\partial \gamma} \\ 0 & \frac{\partial \gamma^1}{\partial \gamma} \end{bmatrix}. \quad (14)$$

We should note that at this point, parameters l and p in (12) have explicit physical meaning and define a virtual reference point with reference to the vehicle platform. They can be selected at will and the details can be clearly seen from the example in Section IV. The steering angles γ^1 and γ^2 are always restricted by the robot mechanism such that their maximums are smaller than 90° . Given this, we may conclude that the regular conditions in Table II can always be satisfied for real mobile robots with restricted mobility.

Suppose that a feasible desired trajectory $q_d(t)$, $\mu_d(t)$ for the mobile robot is prespecified by an open-loop motion planner such that the dynamics (7) and (8) are satisfied for a uniformly bounded input $u_d(t)$, and corresponding uniformly bounded velocity $\mu_d(t)$, i.e.,

$$\dot{q}_d = G(\theta_d, \gamma_d) \mu_d \quad (15)$$

$$\dot{\mu}_d = u_d. \quad (16)$$

Clearly, the desired trajectory can also be expressed in the form of (10) and (12) as

$$z_d = h(q_d). \quad (17)$$

Let us denote the state-tracking error as

$$\begin{aligned} \tilde{q} &= q - q_d \\ \tilde{\mu} &= \mu - \mu_d \end{aligned}$$

and the output-tracking error as

$$\tilde{z} = z - z_d.$$

We have following definitions.

Definition 1: Stable full-state tracking for (7) and (8) to a given moving trajectory $q_d(t)$, $\mu_d(t)$ in (15) and (16) by a feedback control law u in (8) means that, for any $\varepsilon > 0$, there exists a $\delta > 0$ such that, for all $t \geq t^o \geq 0$

$$\left\| \begin{bmatrix} \tilde{q}(t^o) \\ \tilde{\mu}(t^o) \end{bmatrix} \right\| < \delta \Rightarrow \left\| \begin{bmatrix} \tilde{q}(t) \\ \tilde{\mu}(t) \end{bmatrix} \right\| < \varepsilon.$$

Definition 2: Stable output tracking for (10) of (7) and (8) to a given moving trajectory $z_d(t)$ in (17) by a feedback-control law u in (8) means that, for any $\varepsilon > 0$, there exists a $\delta > 0$ such that, for all $t \geq t^o \geq 0$

$$\|\tilde{z}(t^o)\| < \delta \Rightarrow \|\tilde{z}(t)\| < \varepsilon.$$

Since the output function $h(q)$ is an epimorphism, the stable full-state tracking implies stable output tracking. However, the reverse might not be true in general. It is understood that, for a given desired trajectory $z_d(t)$, the generalized states $q_d(t)$ might not be unique, e.g., a straight-line motion of $z_d(t)$ may be caused by forward or backward motion of a mobile robot and corresponds to different solutions of generalized states $q_d(t)$. In the extreme case, the output tracking of $z_d(t)$ may require the solution of generalized states $q_d(t)$ getting out of its admissible range. For instance, steering angle γ is required to have a value out of its physical limitation, such that the output-tracking-control design is not implementable.

In the rest of this paper, the relationship between the full-state tracking problem and the output-tracking problem of nonholonomic wheeled mobile robots is investigated. Mobile dynamic motion is described in terms of state-tracking errors and/or output-tracking errors. Properties of the internal dynamics are obtained and the critical role of the internal dynamics is addressed. We shall show that, under some sufficient conditions, including suitable selection of the parameters in (12) and design of the desired trajectory (15) and (16), full-state tracking of $q_d(t)$ and $\mu_d(t)$ are achieved. Numerical searches are used to extend the analytical investigation on the full-state tracking stability.

III. FULL-STATE TRACKING AND ZERO-DYNAMICS STABILITY

Since the output function $h(q)$ in (12) is constructed such that the decoupling matrix $E(q)$ in (13) is nonsingular, it is possible to find another function $k(q): R^{(3+s)} \rightarrow R^{(3-m)}$, such that the following maps:

$$\begin{bmatrix} \xi_1 \\ \eta \end{bmatrix} = \Phi(q) = \begin{bmatrix} h(q) \\ k(q) \end{bmatrix} \quad (18)$$

and

$$\begin{bmatrix} \xi_1 \\ \xi_2 \\ \eta \end{bmatrix} = \bar{\Phi}(q, \mu) = \begin{bmatrix} h(q) \\ \dot{h}(q) \\ k(q) \end{bmatrix} = \begin{bmatrix} h(q) \\ E(q)\mu \\ k(q) \end{bmatrix} \quad (19)$$

are both diffeomorphisms.

For mobile robots with restricted mobility, the augmented function $k(q)$ can be simply chosen as follows:

$$\eta = k(q) = \begin{bmatrix} \theta \\ \gamma^2 \end{bmatrix}. \quad (20)$$

Furthermore, define an auxiliary control as

$$\tau = \frac{\partial(E(\theta, \gamma)\mu)}{\partial q} G(\theta, \gamma)\mu + E(\theta, \gamma)u. \quad (21)$$

In the new coordinates (ξ_1, ξ_2, η) , the robot dynamics (7) and (8), and output equation (10) are described as

$$\dot{\xi}_1 = \xi_2 \quad (22)$$

$$\dot{\xi}_2 = \tau \quad (23)$$

$$\dot{\eta} = F(\xi_1, \eta)\xi_2 \quad (24)$$

$$z = \xi_1 \quad (25)$$

where

$$F(\xi_1, \eta) = \frac{\partial k(\theta, \gamma)}{\partial q} G(\theta, \gamma) E^{-1}(\theta, \gamma) \Big|_{q=\Phi^{-1}(\xi_1, \eta)}. \quad (26)$$

Similar operations on the desired state lead us to

$$\dot{\xi}_{1d} = \xi_{2d} \quad (27)$$

$$\dot{\xi}_{2d} = \tau_d \quad (28)$$

$$\dot{\eta}_d = F(\xi_{1d}, \eta_d) \xi_{2d} \quad (29)$$

$$z_d = \xi_{1d}. \quad (30)$$

Taking the difference between the above two sets of equations, we obtain the dynamics of tracking errors in terms of $\tilde{\xi} = \xi_i - \xi_{id}$ ($i = 1, 2$) and $\tilde{\eta} = \eta - \eta_d$, and output errors $\tilde{z} = z - z_d$, as follows:

$$\dot{\tilde{\xi}}_1 = \tilde{\xi}_2 \quad (31)$$

$$\dot{\tilde{\xi}}_2 = \tau - \dot{\xi}_{2d} \quad (32)$$

$$\dot{\tilde{\eta}} = \varphi(\tilde{\xi}_1, \tilde{\xi}_2, \tilde{\eta}, t) \quad (33)$$

$$\tilde{z} = \tilde{\xi}_1 \quad (34)$$

where

$$\varphi(\tilde{\xi}_1, \tilde{\xi}_2, \tilde{\eta}, t) = F(\tilde{\xi}_1 + \xi_{1d}(t), \tilde{\eta} + \eta_d(t))(\tilde{\xi}_2 + \xi_{2d}(t)) - F(\xi_{1d}(t), \eta_d(t))\xi_{2d}(t). \quad (35)$$

This set of tracking-error dynamic equations (31)–(34) consists of two parts. The first part is the ξ subsystem (31) and (32) with auxiliary control input τ . This part handles the output-tracking error \tilde{z} . The second part is the η subsystem (33) that is nonautonomous.

The output-tracking problem is a stability problem for the ξ subsystem. The controller design for the stability problem of the ξ subsystem is a partial solution to the full-state stability problem of error dynamic (31)–(33). Different control theories can be applied to this purpose. The simplest candidate is the linear control design method, while sliding mode control, adaptive control and robust control are applicable as well. Generally, control input u in (21) can be designed in such a way that the closed loop of the ξ subsystem is (asymptotically) stable itself and in the following form:

$$\dot{\tilde{\xi}}_1 = \tilde{\xi}_2 \quad (36)$$

$$\dot{\tilde{\xi}}_2 = g(\tilde{\xi}_1, \tilde{\xi}_2). \quad (37)$$

In this case, the η subsystem characterizes the internal dynamics and its stability property determines whether the stable full-state tracking and even the stable output tracking can be achieved. In particular, the zero-dynamics equations (33) and (35) when the system output is set to zero ($\tilde{z} = 0$), are given as

$$\dot{\tilde{\eta}} = \varphi(0, 0, \tilde{\eta}, t) \quad (38)$$

$$= \varphi_o(\tilde{\eta}, t) \quad (39)$$

$$= [F(\xi_{1d}(t), \tilde{\eta} + \eta_d(t)) - F(\xi_{1d}(t), \eta_d(t))] \xi_{2d}(t) \quad (40)$$

and their stability is critical to the internal stability.

To gain more insights to the tracking-error internal dynamics and zero dynamics, we would like to express the tracking-error

internal dynamics (33) and (35), and tracking-error zero dynamics (39) and (40) in terms of the original mobile robot generalized coordinates. To this end, we partition generalized state q to $q_1 \in R^{m+s}$ and $q_2 \in R^{3-m}$ as

$$q_1 = [\zeta^T \ \gamma^1]^T \quad \text{and} \quad q_2 = \eta = [\theta \ \gamma^2]^T.$$

Then, using (26) and $\xi_2 = E(q)\mu$ in (19), (33) and (35) become

$$\dot{\tilde{q}}_2 = f(\tilde{q}_2, \tilde{q}_1, \tilde{\mu}, q_d, \mu_d) \quad (41)$$

$$= \begin{bmatrix} d\theta \\ d\gamma^2 \end{bmatrix} (G(\tilde{q}_1 + q_{1d}, \tilde{q}_2 + q_{2d})(\tilde{\mu} + \mu_d) - G(q_d)\mu_d) \quad (42)$$

where, we have used notions $d\theta$ and $d\gamma^2$ to denote the bases of a covector field $\omega(q)$, with $q = [x \ y \ \theta \ \gamma^1 \ \gamma^2]^T$, corresponding to states θ and γ^2 , respectively. In the same way, (39) and (40) become

$$\dot{\tilde{q}}_2 = f_o(\tilde{q}_2, q_d, \mu_d) \quad (43)$$

$$= \begin{bmatrix} d\theta \\ d\gamma^2 \end{bmatrix} [G(q_{1d}, \tilde{q}_2 + q_{2d})E^{-1}(q_{1d}, \tilde{q}_2 + q_{2d})E(q_d) - G(q_d)]\mu_d. \quad (44)$$

The physical system configurations of the mobile robots with restricted mobility lead to further reduction of arguments in the tracking-error internal dynamics (41) as

$$\dot{\tilde{q}}_2 = f(\tilde{q}_2, \tilde{\gamma}^1, \tilde{\mu}, \gamma_d, \mu_d) \quad (45)$$

and zero dynamics (43) as

$$\dot{\tilde{q}}_2 = f_o(\tilde{q}_2, \gamma_d, \mu_d). \quad (46)$$

It is interesting to note that, in physical systems, γ_d and μ_d are desired steering angles and velocities, respectively, and they are both uniformly bounded by design. This claim can be formally stated in the following Lemma.

Lemma 1: The tracking-error internal dynamics (41) and the tracking-error zero dynamics (43) are independent of posture coordinates (x_d, y_d, θ_d) of the desired trajectory and can be described by (45) and (46), respectively. Moreover, if γ_d and μ_d of the desired trajectory are uniformly bounded, the following hold.

- The function $f(\tilde{q}_2, \tilde{q}_1, \tilde{\mu}, q_d, \mu_d)$ in (41) is Lipschitzian in $(\tilde{q}_1, \tilde{q}_2, \tilde{\mu})$ and uniformly bounded with respect to all $t \geq 0$.
- The function $f_o(\tilde{q}_2, q_d, \mu_d)$ in (43) is Lipschitzian in \tilde{q}_2 and bounded in a neighborhood of $\tilde{\gamma}^2 = 0$ uniformly with respect to all $t \geq 0$.

Proof:

- Independent of posture coordinates** (x_d, y_d, θ_d) :

Based on the structure of (42) and (44), it is clear that the position coordinates $\zeta_d = [x_d \ y_d]^T$ does not appear explicitly. Thus, it is sufficient to show that θ_d does not appear independently. First, we note that

$$\begin{aligned} \begin{bmatrix} d\theta \\ d\gamma^2 \end{bmatrix} G(\theta, \gamma) &= \begin{bmatrix} d\theta \\ d\gamma^2 \end{bmatrix} \begin{bmatrix} R^T(\theta)Q(\gamma) & 0 \\ b^T(\gamma) & 0 \\ 0 & I_s \end{bmatrix} \\ &= \begin{bmatrix} b^T(\gamma) & 0 & 0 \\ 0 & 0_{s+m-2} & I_{2-m} \end{bmatrix} \end{aligned} \quad (47)$$

which is independent of $\theta_d(t)$. Using this fact, (41) becomes

$$\begin{bmatrix} \dot{\tilde{\theta}} \\ \dot{\tilde{\gamma}}^2 \end{bmatrix} = \begin{bmatrix} b^T (\tilde{\gamma}^1 + \gamma_d^1, \tilde{\gamma}^2 + \gamma_d^2) & 0 & 0 \\ 0 & 0 & I_{2-m} \end{bmatrix} (\tilde{\mu} + \mu_d) - \begin{bmatrix} b^T (\gamma_d) & 0 & 0 \\ 0 & 0_{s+m-2} & I_{2-m} \end{bmatrix} \mu_d \quad (48)$$

which is in the form of (45).

Secondly, noting (13), we have

$$\begin{aligned} E(q_{1d}, \tilde{q}_2 + q_{2d}) &= \begin{bmatrix} R^T(\tilde{\theta} + \theta_d) & 0 \\ 0 & I_{m+s-2} \end{bmatrix} \bar{E}(\gamma_d^1, \tilde{\gamma}^2 + \gamma_d^2) \\ E(q_d) &= \begin{bmatrix} R^T(\theta_d) & 0 \\ 0 & I_{m+s-2} \end{bmatrix} \bar{E}(\gamma_d). \end{aligned}$$

Because the rotation matrix $R(\theta)$ is an orthogonal matrix, the inverse of $E(q_{1d}, \tilde{q}_2 + q_{2d})$ is

$$\begin{aligned} E^{-1}(q_{1d}, \tilde{q}_2 + q_{2d}) &= \bar{E}^{-1}(\gamma_d^1, \tilde{\gamma}^2 + \gamma_d^2) \begin{bmatrix} R(\tilde{\theta} + \theta_d) & 0 \\ 0 & I_{m+s-2} \end{bmatrix}. \quad (49) \end{aligned}$$

Furthermore

$$R(\tilde{\theta} + \theta_d) R^T(\theta_d) = R(\tilde{\theta}).$$

The matrix $E^{-1}(q_{1d}, \tilde{q}_2 + q_{2d})E(q_d)$ is obtained as follows:

$$\begin{aligned} E^{-1}(q_{1d}, \tilde{q}_2 + q_{2d}) E(q_d) &= \bar{E}^{-1}(\gamma_d^1, \tilde{\gamma}^2 + \gamma_d^2) \begin{bmatrix} R(\tilde{\theta}) & 0 \\ 0 & I_{m+s-2} \end{bmatrix} \bar{E}(\gamma_d) \quad (50) \end{aligned}$$

which is clearly independent of the orientation coordinate θ_d . Using (50) together with (47), (43) becomes

$$\begin{aligned} \begin{bmatrix} \dot{\tilde{\theta}} \\ \dot{\tilde{\gamma}}^2 \end{bmatrix} &= f(\tilde{q}_2, \gamma_d, \mu_d) \\ &= \begin{bmatrix} b^T (\gamma_d^1, \tilde{\gamma}^2 + \gamma_d^2) & 0 & 0 \\ 0 & 0_{s+m-2} & I_{2-m} \end{bmatrix} \cdot \bar{E}^{-1}(\gamma_d^1, \tilde{\gamma}^2 + \gamma_d^2) \begin{bmatrix} R(\tilde{\theta}) & 0 \\ 0 & I_{m+s-2} \end{bmatrix} \bar{E}(\gamma_d) \mu_d \\ &\quad - \begin{bmatrix} b^T (\gamma_d) & 0 & 0 \\ 0 & 0_{s+m-2} & I_{2-m} \end{bmatrix} \mu_d \quad (51) \end{aligned}$$

which is in the form (46).

2) Lipschitzian and boundedness:

By the definition of matrix $Q(\gamma)$ and vectors $b(\gamma)$ and $d(\gamma)$ in Tables I and II, they are all Lipschitz continuous and uniformly bounded. Observing the structure of the tracking-error internal dynamics (48) and the tracking-error zero dynamics (51), and noting the boundedness of both γ_d and μ_d , and the boundedness of $\bar{E}^{-1}(\gamma_d^1, \tilde{\gamma}^2 + \gamma_d^2)$ in (51) in a neighborhood of $\tilde{\gamma}^2 = 0$, the claim of Lipschitzian and boundedness for functions $f(\tilde{q}_2, \tilde{q}_1, \tilde{\mu}, q_d, \mu_d)$ and $f_o(\tilde{q}_2, q_d, \mu_d)$ is established.

This completes the proof. \square

At this point, we may give a main result by the following theorem.

Theorem 1: Consider the mobile robots with restricted mobility described by (7) and (8) with a moving desired trajectory $(q_d(t), \mu_d(t))$ satisfying (15) and (16) with γ_d and μ_d uniformly bounded. Suppose that control input u in (21) is specified such that, by using the transformation (19), the closed-loop ξ sub-system is in the form of (36) and (37) and is stable. Then, the uniformly asymptotic stability of tracking-error zero dynamics (46) implies the stable full-state tracking of (7) and (8) to desired trajectory (15) and (16).

Proof: Under (19), function $f(\tilde{q}_2, \tilde{q}_1, \tilde{\mu}, q_d, \mu_d)$ in (41) is Lipschitzian in $(\tilde{q}_1, \tilde{q}_2, \tilde{\mu})$ uniformly with respect to all $t \geq 0$ is equivalent to that function $\varphi(\tilde{\xi}_1, \tilde{\xi}_1, \tilde{\eta}, t)$ is Lipschitzian in $(\tilde{\xi}_1, \tilde{\xi}_1, \tilde{\eta})$ uniformly with respect to all $t \geq 0$. Meanwhile, the uniformly asymptotic stability of tracking-error zero dynamics (46) is equivalent to that of tracking-error zero dynamics (39). Then, the claim in Theorem 1 is proved by following Lemma 2 in the Appendix. \square

In case the output-tracking control law is used, Theorem 1 offers sufficient conditions for stable full-state tracking and thus, stable output tracking in a neighborhood of $\tilde{q}_2 = 0$. However, it should be pointed out that the opposite is not true, i.e., stable output tracking does not imply stable full-state tracking. The following two scenarios illustrate this situation.

In the cases of $m = 2$, i.e., type (2, 0) and type (2, 1) mobile robots, the admissible solution range of internal state θ is not bounded. The internal-state tracking error \tilde{q}_2 might not converge while stable-output tracking might still be possible. An example of the type (2, 0) mobile robot is given in [17], the instability of backward tracking (indeed, the full-state tracking fails) occurs while the mobile robot exhibits a swiveling motion such that the stable output tracking is achieved.

In the cases of $m = 1$, i.e., type (1, 1) and type (1, 2) mobile robots, the admissible solution range of the internal state is bounded ($|\gamma^2| < \gamma_{\max}^2 < \pi/2$), the divergence of the error internal state $\tilde{\gamma}^2$ will cause the failures of both the output tracking and the full-state tracking. However, in some special cases, it is still possible that stable-output tracking is achieved while the stable full-state tracking fails. For example, a straight-line trajectory can be stably tracked by a forward motion (corresponding to internal state errors $\tilde{\gamma}^2 = 0$ and $\tilde{\theta} = 0$). The same straight-line trajectory can also be followed by a backward motion [corresponding to the internal state error $\tilde{\gamma}^2 = 0$ and another internal state error $\tilde{\theta} = \pi$ (instability at $\tilde{\theta} = 0$)].

Compared with an existing result of [18, Proposition 5], Theorem 1 covers a wider class of desired trajectory. In [18, Proposition 5], the condition that $\dot{z}_{1zef}(t)$ must be L_1 is so restrictive that a straight drive forward cannot meet the requirement. Furthermore, the results offered in [18, Proposition 5] can only ensure the internal state z_3 being bounded for every t , which is not stability.

In general, especially when $m = 1$, this tracking-error zero dynamics (46) is highly complex and stability analysis is very difficult. Here, we give another main result in the following theorem. Linear approximation is used to determine the stability of the nonautonomous tracking-error zero dynamics (46).

Theorem 2: Suppose $\gamma_d(t)$, $\mu_d(t)$ and $u_d(t)$ are uniformly bounded. The following first-order approximation:

$$\dot{\tilde{q}}_2 = A(\gamma_d, \mu_d)\tilde{q}_2 \quad (52)$$

where

$$A(\gamma_d, \mu_d) = \left[\frac{\partial f_o(\tilde{q}_2, \gamma_d, \mu_d)}{\partial \tilde{q}_2} \right]_{\tilde{q}_2=0}$$

is the linear approximation of (46). Furthermore, if the linear-approximation system (52) for every frozen $(\gamma_d(t), \mu_d(t)) = (\bar{\gamma}_d, \bar{\mu}_d)$ is exponentially stable in a neighborhood of $\tilde{\gamma}^2 = 0$, (46) is uniformly asymptotically stable.

Proof: Firstly, note that $\tilde{q}_2 = 0$ is the equilibrium of (46). Taylor expansion of function $f_o(\tilde{q}_2, \gamma_d, \mu_d)$ can be expressed as

$$f_o(\tilde{q}_2, \gamma_d, \mu_d) = A(\gamma_d, \mu_d)\tilde{q}_2 + f_{h.o.t.}(\tilde{q}_2, \gamma_d, \mu_d).$$

Define $f_{h.o.t.}(\tilde{q}_2, \gamma_d, \mu_d)$ to be the higher order terms

$$f_{h.o.t.}(\tilde{q}_2, \gamma_d, \mu_d) = f_o(\tilde{q}_2, \gamma_d, \mu_d) - A(\gamma_d, \mu_d)\tilde{q}_2.$$

Due to both $\gamma_d(t)$ and $\mu_d(t)$ being uniformly bounded, Lemma 1 shows $f_o(\tilde{q}_2, \gamma_d, \mu_d)$ is Lipschitzian in \tilde{q}_2 uniformly with respect to all $t \geq 0$. Its first approximation $A(\gamma_d, \mu_d)\tilde{q}_2$ must be also Lipschitzian in \tilde{q}_2 uniformly with respect to all $t \geq 0$. Given this, we conclude that

$$\limsup_{\|\tilde{q}_2\| \rightarrow 0} \frac{\|f_{h.o.t.}(\tilde{q}_2, \gamma_d, \mu_d)\|}{\|\tilde{q}_2\|} = 0 \quad \forall t \geq 0. \quad (53)$$

Therefore, Lemma 3 in the Appendix implies that (52) is the linear approximation of nonautonomous zero dynamics system (46), and its uniformly asymptotic stability implies sufficiently to the uniformly asymptotic stability of (46).

Secondly, since $\gamma_d(t)$, $\mu_d(t)$ is uniformly bounded such that, $f_o(\tilde{q}_2, \gamma_d, \mu_d)$ is Lipschitzian in \tilde{q}_2 and bounded in a neighborhood of $\tilde{\gamma}^2 = 0$ uniformly with respect to all $t \geq 0$ as shown in Lemma 1, $A(\gamma_d, \mu_d)$ is Lipschitz continuous uniformly in γ_d, μ_d and uniformly bounded in a neighborhood of $\tilde{\gamma}^2 = 0$ to all $t \geq 0$. Furthermore, since both $\dot{\gamma}_d(t) = \omega_d(t) \in \mu_d$ and $\dot{\mu}_d(t) = u_d(t)$ are also uniformly bounded, the linear-approximation system (52) satisfies the assumptions in Lemma 5 in the Appendix if the linear-approximation system (52) for every frozen $(\gamma_d(t), \mu_d(t)) = (\bar{\gamma}_d, \bar{\mu}_d)$ is exponentially stable. Thus, the linear-approximation system (52) is uniformly exponentially stable using Lemma 5.

Using the above two facts, this claim in Theorem 2 is proved. \square

IV. TRACKING STABILITY OF A CAR-LIKE ROBOT

The stability-analysis method proposed in the previous section is generally suitable for analyzing the trajectory tracking stability of any wheeled mobile robot under an output-tracking control scheme. Without loss of generality, we investigate a car-like robot in details. A car-like robot has the least mobility ($m = 1$) and the stability analysis for a car-like robot is one of the most challenging problems among the nonholonomic wheeled mobile robots.

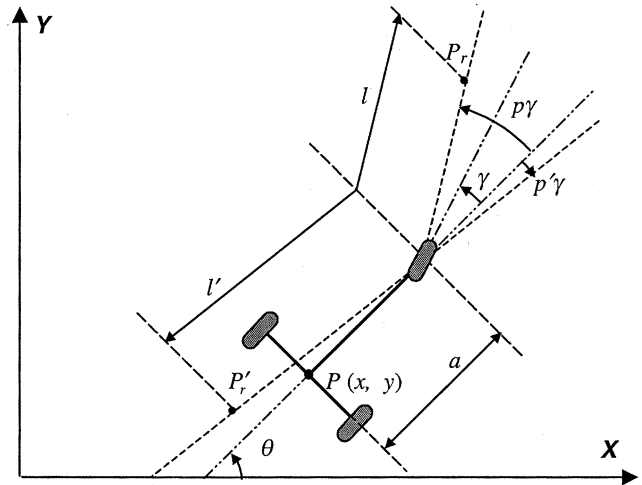


Fig. 2. Car-like robot configuration with virtual reference points.

A rear wheel driving car-like robot, as shown in Fig. 2, is a type (1, 1) mobile robot with restricted mobility and is modeled by (7) and (8) with

$$q = \begin{bmatrix} x \\ y \\ \theta \\ \gamma \end{bmatrix} \quad G(q) = \begin{bmatrix} \cos \theta & 0 \\ \sin \theta & 0 \\ \frac{1}{a} \tan \gamma & 0 \\ 0 & 1 \end{bmatrix} \quad (54)$$

$$\mu = \begin{bmatrix} v \\ \omega \end{bmatrix} \quad u = \begin{bmatrix} u_m \\ u_s \end{bmatrix}$$

where, the triplet (x, y, θ) is the posture; γ is the steering angle; v is the longitudinal velocity; ω is the steering rate; u_m and u_s are control inputs that are homogeneous to actual motor torques; and a is a positive constant of the wheelbase.

The output function (10) is chosen as

$$z = h(q) = \begin{bmatrix} x + a \cos \theta + l \cos(\theta + p\gamma) \\ y + a \sin \theta + l \sin(\theta + p\gamma) \end{bmatrix}. \quad (55)$$

It represents the coordinates of a virtual reference point. When parameters l and p are both positive, the output $h(q)$ defines a virtual reference point P_r in front of the vehicle as shown in Fig. 2. When parameters l and p are both negative, the output $h(q)$ defines a virtual reference point P'_r behind the vehicle's front axle as shown in Fig. 2. To study the zero dynamics, select the augmented function $k(q)$ in (20) as

$$\eta = q_2 = k(q) = [\theta \quad \gamma]^T. \quad (56)$$

It is easy to check that the transformation (18) and (19) are diffeomorphisms if

$$\det \left(\frac{\partial \bar{\Phi}(q, \mu)}{\partial [q^T \quad \mu^T]^T} \right) = \frac{lp \cos(p\gamma - \gamma)}{\cos \gamma} \neq 0 \quad (57)$$

which is true if

$$lp \neq 0, \quad \text{and} \quad |1 - p| < \frac{\pi}{2\gamma_{\max}}, \quad \text{and} \quad |\gamma| \leq \gamma_{\max} < \frac{\pi}{2}. \quad (58)$$

Condition $lp \neq 0$ implies that the virtual reference point P_r cannot be fixed on the robot ($l = 0$), or on the symmetric axle ($p = 0$) of the car-like robot. Limitation for the steering angle $|\gamma| \leq \gamma_{\max} < \pi/2$ is always satisfied in a real car-like robot. With the above developments, the tracking-error zero dynamics of a car-like robot is obtained as, a special form of (46)

$$\begin{bmatrix} \dot{\tilde{\theta}} \\ \dot{\tilde{\gamma}} \end{bmatrix} = \begin{bmatrix} f_1(\tilde{\theta}, \tilde{\gamma}, \gamma_d, v_d, \omega_d) \\ f_2(\tilde{\theta}, \tilde{\gamma}, \gamma_d, v_d, \omega_d) \end{bmatrix} \quad (59)$$

with (60) and (61), as shown at the bottom of the page where, $\tilde{\theta} = \theta - \theta_d$ and $\tilde{\gamma} = \gamma - \gamma_d$. The tracking-error zero dynamics (59) is highly nonlinear and depends on not only variables (γ_d, v_d, ω_d) given in the desired trajectory but also parameters (l, p) that define the virtual reference point. However, (59) is independent of the posture vector $\xi_d = [x_d, y_d, \theta_d]^T$ given in the desired trajectory. To use Theorem 2, the linear approximation of (59) at equilibrium $\tilde{q}_2 = [\tilde{\theta} \ \tilde{\gamma}]^T = 0$ is derived, with the help of the software package—MAPLE, as follows:

$$\begin{aligned} \dot{\tilde{q}}_2 &= A(\gamma_d, v_d, \omega_d) \tilde{q}_2 \\ &= \begin{bmatrix} a_{11}(\gamma_d, v_d, \omega_d) & a_{12}(\gamma_d, v_d, \omega_d) \\ a_{21}(\gamma_d, v_d, \omega_d) & a_{22}(\gamma_d, v_d, \omega_d) \end{bmatrix} \tilde{q}_2 \end{aligned} \quad (62)$$

with the equations shown at the bottom of the page. The linear approximation (62) has five parameters ($\gamma_d, v_d, \omega_d, l$, and p). It is so complex that its eigenvalues analytic studies are, in gen-

eral, difficult, if not impossible. However, in some special cases, eigenvalues analysis can offer more insights. One such case is given as follows.

Theorem 3: The tracking-error zero dynamics (59) is uniformly asymptotically stable if the following conditions are satisfied:

- $p = 1$ and $l > 0$;
- $0 < v_d < V$ and $|\gamma_d| < \gamma_{\max}$ for constant $V > 0$ and $0 < \gamma_{\max} < \pi/2$.

Proof: By setting $p = 1$, the linear approximation (62) is simplified with

$$\begin{aligned} A(\gamma_d, v_d) &= v_d \begin{bmatrix} 0 & \frac{1}{a} \\ -\frac{1}{l \cos \gamma_d} & -\frac{1}{l \cos \gamma_d} - \frac{1}{a} \end{bmatrix} \\ &+ \frac{l}{a^2} \sin \gamma_d (v_d \tan \gamma_d + a \omega_d) \begin{bmatrix} 1 & 1 \\ -1 & -1 \end{bmatrix}. \end{aligned} \quad (63)$$

Clearly, $A(\gamma_d, v_d)$ is Lipschitz continuous and uniformly bounded under the conditions a) and b). Furthermore, its eigenvalues at every frozen $(\bar{\gamma}_d, \bar{v}_d)$ are

$$\lambda_1 = -\frac{\bar{v}_d}{a} \quad \lambda_2 = -\frac{\bar{v}_d}{l \cos \bar{\gamma}_d} \quad (64)$$

and both of them are negative. Application of Theorem 2 in this case leads to the conclusion that (59) is uniformly asymp-

$$f_1 = \frac{v_d \sin(\tilde{\gamma} + \gamma_d) \left(\cos(\tilde{\theta} + p\tilde{\gamma} + (p-1)\gamma_d) + \frac{l}{a} \sin \gamma_d \sin(\tilde{\theta} + p\tilde{\gamma}) \right)}{a \cos \gamma_d \cos((p-1)\tilde{\gamma} + (p-1)\gamma_d)} - \frac{v_d}{a} \tan \gamma_d + \frac{pl\omega_d \sin(\tilde{\gamma} + \gamma_d) \sin(\tilde{\theta} + p\tilde{\gamma})}{a \cos((p-1)\tilde{\gamma} + (p-1)\gamma_d)} \quad (60)$$

$$\begin{aligned} f_2 &= \frac{-av_d \sin(\tilde{\theta} + \tilde{\gamma}) + lv_d \sin \gamma_d \cos(\tilde{\theta} + \tilde{\gamma} - (p-1)\gamma_d)}{pla \cos \gamma_d \cos((p-1)\tilde{\gamma} + (p-1)\gamma_d)} - \frac{v_d \sin(\tilde{\gamma} + \gamma_d) \left(\cos(\tilde{\theta} + p\tilde{\gamma} + (p-1)\gamma_d) + \frac{l}{a} \sin \gamma_d \sin(\tilde{\theta} + p\tilde{\gamma}) \right)}{ap \cos \gamma_d \cos((p-1)\tilde{\gamma} + (p-1)\gamma_d)} \\ &+ \frac{a\omega_d \cos(\tilde{\theta} + \tilde{\gamma} - (p-1)\gamma_d) - l\omega_d \sin(\tilde{\gamma} + \gamma_d) \sin(\tilde{\theta} + p\tilde{\gamma})}{a \cos((p-1)\tilde{\gamma} + (p-1)\gamma_d)} - \omega_d \end{aligned} \quad (61)$$

$$a_{11}(\gamma_d, v_d, \omega_d) = \frac{2v_d l \sin^2 \gamma_d - v_d a \cos(p\gamma_d - 2\gamma_d) + v_d a \cos(p\gamma_d) + pl a \omega_d \sin(2\gamma_d)}{a^2 (\cos(p\gamma_d - 2\gamma_d) + \cos \gamma_d)}$$

$$a_{12}(\gamma_d, v_d, \omega_d) = \frac{2v_d pl \sin^2 \gamma_d + 2v_d a \cos(p\gamma_d) + p^2 l a \omega_d \sin(2\gamma_d)}{a^2 (\cos(p\gamma_d - 2\gamma_d) + \cos \gamma_d)}$$

$$\begin{aligned} a_{21}(\gamma_d, v_d, \omega_d) &= -2v_d \frac{l^2 \sin^2 \gamma_d + a^2 - la \cos(p\gamma_d - 2\gamma_d) + la \cos(p\gamma_d)}{pla^2 (\cos(p\gamma_d - 2\gamma_d) + \cos \gamma_d)} \\ &- \omega_d \frac{l \sin(2\gamma_d) - a \sin(p\gamma_d) - a \sin(p\gamma_d - 2\gamma_d)}{a (\cos(p\gamma_d - 2\gamma_d) + \cos \gamma_d)} \end{aligned}$$

$$\begin{aligned} a_{22}(\gamma_d, v_d, \omega_d) &= -v_d \frac{2pl^2 \sin^2 \gamma_d + 2a^2 - pla \cos(p\gamma_d - 2\gamma_d) + la(2+p) \cos(p\gamma_d)}{pla^2 (\cos(p\gamma_d - 2\gamma_d) + \cos \gamma_d)} \\ &- \omega_d \frac{pl \sin(2\gamma_d) - pa \sin(p\gamma_d) - pa \sin(p\gamma_d - 2\gamma_d)}{a (\cos(p\gamma_d - 2\gamma_d) + \cos \gamma_d)} \end{aligned}$$

totically stable under the conditions a) and b). The proof is completed. \square

Theorem 3 gives the sufficient condition of the stable full-state tracking when a car-like robot tracks a feasible trajectory that is confined to move forward ($v_d > 0$). For a feasible trajectory, condition $|\gamma_d| < \gamma_{\max} < \pi/2$ always holds. In this case, the output should be suitably selected such that, the virtual reference point P_r is in front of the front wheel axle ($l > 0$) in the steering direction ($p = 1$).

On the other hand, the instability conditions of the tracking-error zero dynamics can be established using the linear approximation for some typical maneuvers. One such simple motion is that the vehicle is moving with the desired velocity at a constant speed v_d and the desired steering angle is zero, $\gamma_d = 0$, and tracking instability occurs when the virtual reference point is chosen in certain area as stated in the following theorem.

Theorem 4: Suppose $\gamma_d = 0$, then (59) is unstable in the following situations:

driving forward: if $v_d = V$, where $V > 0$, and either a) $lp < 0$ or b) $lp > 0$ and $l < -a$;

driving backward: If $v_d = -V$, where $V > 0$, and either a) $lp < 0$ or b) $lp > 0$ and $l > -a$.

Proof: When $\gamma_d = 0$, the linear approximation (62) is simplified as

$$\dot{\tilde{q}}_2 = A(v_d) \tilde{q}_2 \quad (65)$$

with

$$A(v_d) = v_d \begin{bmatrix} 0 & \frac{1}{a} \\ -\frac{1}{pl} & -\frac{1}{p} \left(\frac{1}{a} + \frac{1}{l} \right) \end{bmatrix}. \quad (66)$$

For constant desired velocity $v_d = V$ or $v_d = -V$, $A(v_d)$ is constant. The eigenvalues of (66) are obtained as

$$\lambda_{1,2} = \frac{v_d}{2pla} \left(-a - l \pm \sqrt{(a+l)^2 - 4pla} \right) \quad (67)$$

where, the wheelbase a is a positive constant. The tracking-error zero dynamics (59) is unstable if at least one of eigenvalues (67) has a positive real part.

Driving forward: The condition a) leads to $\sqrt{(a+l)^2 - 4pla} > |a+l|$ and

$$\lambda_2 = \frac{V}{2pla} \left(-a - l - \sqrt{(a+l)^2 - 4pla} \right) > 0. \quad (68)$$

Alternatively, the condition b) leads to $Re \left(-a - l + \sqrt{(a+l)^2 - 4pla} \right) > 0$ and

$$Re(\lambda_1) = \frac{V}{2pla} Re \left(-a - l + \sqrt{(a+l)^2 - 4pla} \right) > 0. \quad (69)$$

Driving backward: The condition a) leads to $\sqrt{(a+l)^2 - 4pla} > |a+l|$ and

$$\lambda_1 = \frac{-V}{2pla} \left(-a - l + \sqrt{(a+l)^2 - 4pla} \right) > 0. \quad (70)$$

Alternatively, the condition b) leads to $Re \left(-a - l - \sqrt{(a+l)^2 - 4pla} \right) < 0$ and

$$Re(\lambda_2) = \frac{-V}{2pla} Re \left(-a - l - \sqrt{(a+l)^2 - 4pla} \right) > 0. \quad (71)$$

All these conclude that the tracking-error zero dynamics is unstable using Lemma 4 in the Appendix. This completes the proof. \square

This theorem gives the divergence conditions of the internal states $[\tilde{\theta} \ \tilde{\gamma}]^T$ when the desired trajectory is a straight motion and the output-tracking error is forced to be zero. In these cases, stable full-state tracking cannot be achieved even though stable output tracking is still possible. For instance, if the trajectory is a straight ($\gamma_d = 0$) backward ($v_d = -V < 0$) motion along X -axis ($\theta = 0$), and the output function is selected such that $p = 1$ and $l > 0$, solution ($\tilde{x} = 2(a+l)$, $\tilde{y} = 0$, $\tilde{\theta} = \pi$, $\tilde{\gamma} = 0$) ensures stable output tracking ($\tilde{z} = 0$) but not stable full-state tracking ($\tilde{x} \neq 0$, $\tilde{\theta} \neq 0$).

V. FURTHER STABILITY ANALYSIS BY NUMERICAL SEARCH

Due to the complexity of the tracking-error zero dynamics, analytical investigation of the stable full-state tracking problem faces limitation. To further investigate the stable full-state tracking problem in addition to the sufficient conditions provided in Theorem 3, we use numerical search to explore the sets of five design parameters ($v_d, \omega_d, \gamma_d, l, p$) that ensure the full-state tracking stability.

The numerical analysis is based on Theorem 2 and its application to the car-like robot case where (59) is associated with the linear approximation (62). For any feasible trajectory, the parameters γ_d, ω_d and v_d are all uniformly bounded by design. Theorem 2 implies that the tracking-error zero dynamics (59) is uniformly asymptotically stable if its linear approximation (62) is asymptotically stable uniformly in every frozen $(\bar{\gamma}_d, \bar{\omega}_d, \bar{v}_d)$. We know that the design parameters (l, p) are important in the tracking stability of the tracking-error zero dynamics (59). To find the sets of the design parameters (l, p) that ensure the stable full-state tracking, the eigenvalues of the matrix $A(\gamma_d, v_d, \omega_d)$ of the linear approximation (62) are numerically evaluated for certain frozen triplet $(\bar{\gamma}_d, \bar{\omega}_d, \bar{v}_d)$. Negative real parts of all eigenvalues indicate the exponential stability of the linear approximation (62) for that particular set of parameter values (l, p) . Searching for all such sets of parameter values of exponential stability lead us to the sets of parameter values that ensure the stable full-state tracking. The numerical analysis for searching such sets of parameter values (l, p) for certain desired trajectories $(\bar{\gamma}_d, \bar{\omega}_d, \bar{v}_d)$ is proceeded in three cases, i.e., the look-ahead case, the look-below case, and the look-behind case.

Look-Ahead Case: Suppose that the desired trajectory is confined to move forward ($v_d > 0$) at certain velocities and make turns ($\gamma_d \neq 0$) at certain rate, e.g., ($-20 \text{ rad/s} < \omega_d < 20 \text{ rad/s}$). The parameter values $l > 0$ and $p > 0$ indicate that the virtual reference point is located in front of the front axle or is "look ahead." In Fig. 3, the shaded areas are the sets of locations of the virtual reference points that are

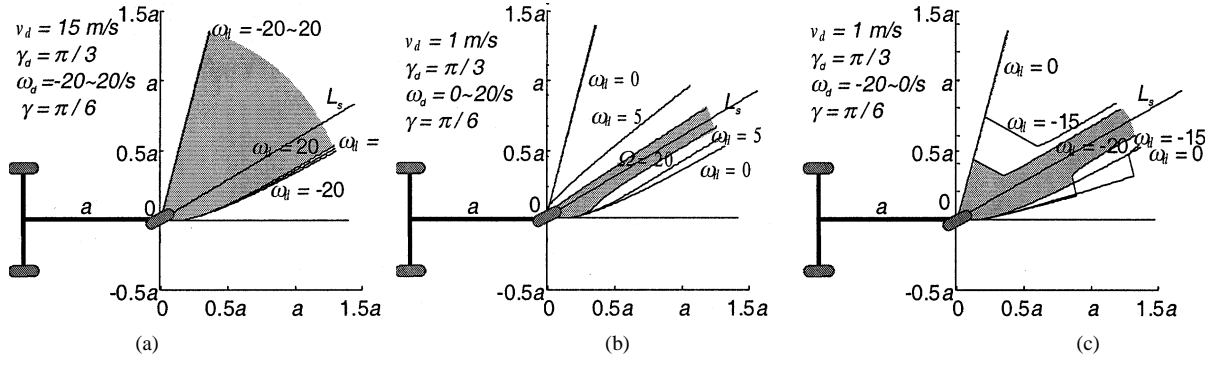
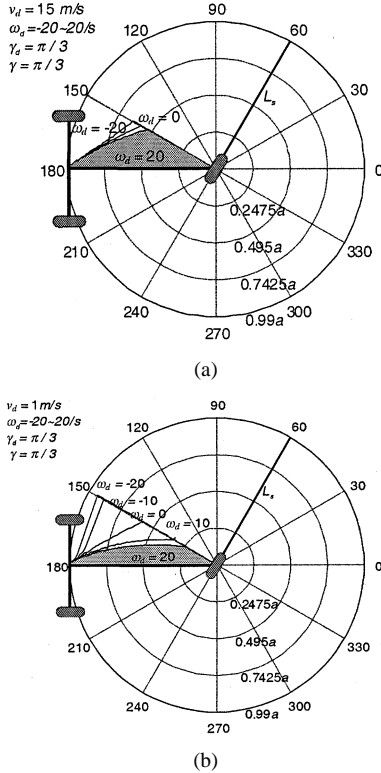

 Fig. 3. Forward moving and “look-ahead” stable sets of virtual reference points. (a) High speed. (b) Low speed ($\gamma_d \omega_d > 0$). (c) Low speed ($\gamma_d \omega_d < 0$).


Fig. 4. Forward moving and “look-behind” stable sets of virtual reference points. (a) High speed. (b) Low speed.

able to ensure the stable full-state tracking at different setting of $(\bar{\gamma}_d, \bar{\omega}_d, \bar{v}_d)$. Comparing Fig. 3(a) with (b) and (c) indicates that higher forward velocity comes with a larger set of such parameter values (l, p) . Fig. 3(b) and (c) shows that higher steering rates come with smaller sets of such parameter values (l, p) . As the limit when steering rate increases, only the fold line L_s ($l > 0$ and $p = 1$) offers the locations being able to ensure the tracking stability as stated in Theorem 3.

Look-Below Case: Suppose that the desired trajectory is confined to move forward ($v_d > 0$) at certain velocities and make turns ($\gamma_d \neq 0$) at a certain rate, e.g., $(-20 \text{ rad/s} < \omega_d < 20 \text{ rad/s})$. The parameter values $-a < l < 0$ and $p < 0$ indicate that the virtual reference point is located below the vehicle or is “look below.” In Fig. 4, the shaded areas are the sets of locations of the virtual reference points that are able to ensure the stable full-state tracking at different setting of $(\bar{\gamma}_d, \bar{\omega}_d, \bar{v}_d)$. Comparing Fig. 4(a) with (b)

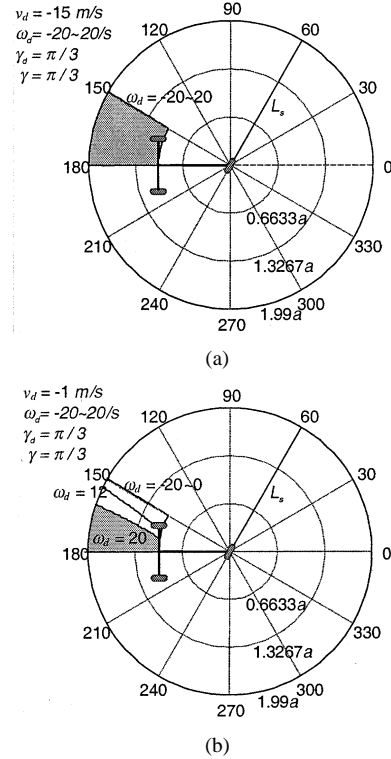


Fig. 5. Forward moving and “look-behind” stable sets of virtual reference points. (a) High speed. (b) Low speed.

indicates that higher forward velocity comes with a larger set of such parameter values (l, p) . Fig. 4(b) shows that higher steering rates come with smaller sets of such parameter values (l, p) . As the steering rate increases, the shaded area converges to the vehicle’s symmetric axis ($-a < l < 0$ and $p = 0$) but the limit is a null set.

Look-Behind Case: Suppose that the desired trajectory is confined to move backward ($v_d < 0$) at certain velocities and make turns ($\gamma_d \neq 0$) at certain rate, e.g., $(-20 \text{ rad/s} < \omega_d < 20 \text{ rad/s})$. The parameter values $l < -a$ and $p > 0$ indicate that the virtual reference point is located behind of the rear axle or “look behind.” In Fig. 5, the shaded areas are the sets of locations of the virtual reference points that are able to ensure the stable full-state tracking at different setting of $(\bar{\gamma}_d, \bar{\omega}_d, \bar{v}_d)$. Comparing Fig. 5(a) with (b) indicates that higher forward velocity comes with a larger set of such parameter values (l, p) . Fig. 5(b) shows that higher steering rates come with smaller sets of such parameter values (l, p) .

Note that these sets of virtual reference points are open sets and the boundaries do not guarantee the full-state tracking stability. As steering rate increases, the shade area converges to the vehicle's symmetric axis ($l < -a$ and $p = 0$) but the limit is a null set. Our intuition and experience verify that driving a car backward with higher steering rates will cause difficulties and even instability.

Some more observations can be made from the above numerical searching results using the following definitions of curvature $k_d(t)$ and curvature change rate $\dot{k}_d(t)$ of the desired trajectory. The curvature of a desired trajectory at time t is given as

$$k_d(t) = \frac{\tan |\gamma_d(t)|}{a} \quad (72)$$

and the corresponding curvature change rate is given as

$$\dot{k}_d(t) = \frac{\omega_d(t) \text{sign}(\gamma_d(t))}{a \cos^2 \gamma_d(t)}. \quad (73)$$

It is clear that larger steering angle $\gamma_d(t)$ leads to larger curvature $k_d(t)$ and that higher steering rate $\omega_d(t) \text{sign}(\gamma_d(t))$ and/or larger steering angle $\gamma_d(t)$ lead to higher curvature change rate $\dot{k}_d(t)$. Furthermore, the curvature change rate $\dot{k}_d(t)$ is positive if the steering angle and the steering rate are in the same directions or $\omega_d(t)\gamma_d(t) > 0$. Otherwise, the curvature change rate $\dot{k}_d(t)$ is negative if the steering angle and the steering rate are in the opposite directions or $\omega_d(t)\gamma_d(t) < 0$. Based on these two indicators, Figs. 3–5 offer the following observations.

- 1) The stable sets of the virtual reference points are smaller when the desired trajectory is in lower velocity and higher curvature change rate.
- 2) The stable sets converge to the fold line (look-ahead) or vehicle symmetric axis (look-below) or its extension (look-behind). The convergences toward the limits occur under the trends of the desired velocity tending to zero and the desired curvature change rate tending to infinity.

VI. SIMULATION RESULTS

The simulation study in this section is based on the car-like robot discussed in Section IV. The desired trajectory, as shown in Fig. 6, consists of three straight lines and two curves. The first curve C_1 is designed with a maximum curvature $k_{\max} = 0.5238$ and a maximum curvature change rate $\dot{k}_{\max} = 0.6864$. The second curve C_2 has a higher maximum curvature $k_{\max} = 0.8479$ and a much higher curvature change rate $\dot{k}_{\max} = 1.7599$. Based on the analysis in the previous sections, it is expected that the second curve is a more difficult manoeuvre and the stable set of virtual reference points is smaller.

In the following, three results are presented and they verify the analysis and conclusions made in the previous sections. The virtual reference points will be chosen based on Theorem 3 and the numerical search results. The vehicle controller is a set of control laws that consist of an input–output feedback linearization [with the output function defined in (55)] control law and a PD control law. With proper selection of the virtual reference point, we can ensure the tracking-error zero dynamics to be asymptotically stable and thus the full-state tracking performance of the vehicle.

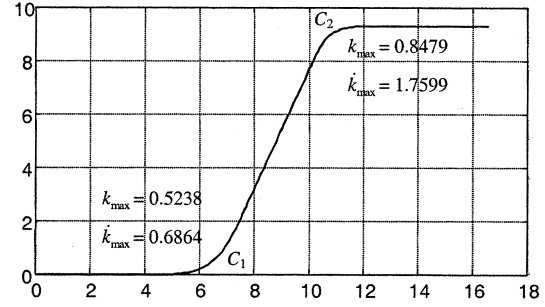


Fig. 6. Desired trajectory.

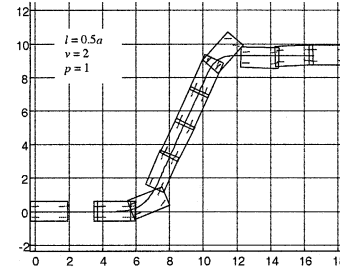
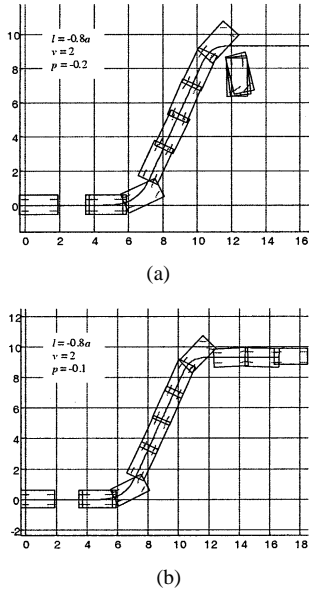
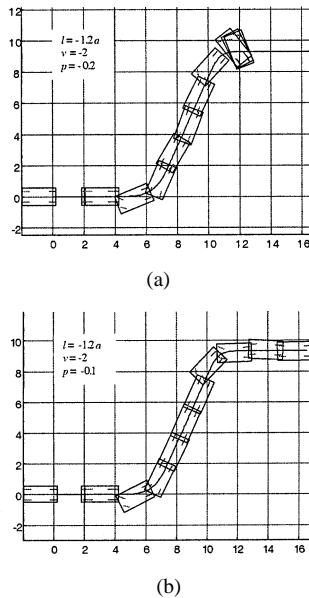


Fig. 7. Look-ahead tracking.

Look-ahead case: In this case, the vehicle is expected to move forward with the desired velocity of $v_d = 2$ meter/second. The virtual reference point is chosen at $P_0 = (l, p) = (0.5a, 1)$ on the steering fold line. Based on Theorem 3, the tracking-error zero dynamics is asymptotically stable and so is the vehicle tracking. The simulation result, as shown in Fig. 7, confirms that the vehicle follows the desired trajectory through out.

Look-below case: In this case, the vehicle is expected to move forward with the same desired velocity of $v_d = 2$ meter/second. The virtual reference point is chosen at two different locations $P_1 = (l, p) = (-0.8a, -0.2)$ and $P_2 = (l, p) = (-0.8a, -0.1)$. Based on Fig. 4, P_2 is closer to the vehicle symmetric axis line and able to handle more difficult maneuvers, such as curve C_2 which has a higher maximum curvature change rate. The simulation results, as shown in Fig. 8, show that, with $p = -0.2$, the vehicle fails to track the desired trajectory at the curve C_2 , and that, with $p = -0.1$, the vehicle succeeds in tracking the complete desired trajectory.

Look-behind case: In this case, the vehicle is turned around and expected to move backward to track the same trajectory with the desired velocity of $v_d = -2$ meter/second. The virtual reference point is chosen at two different locations $P_3 = (l, p) = (-1.2a, -0.2)$ and $P_4 = (l, p) = (-1.2a, -0.1)$. Based on Fig. 5, P_4 is closer to the vehicle symmetric axis line and able to handle more difficult maneuvers, such as curve C_2 which has a higher maximum curvature change rate. The simulation results, as shown in Fig. 9, show that, with $p = -0.2$, the vehicle fails to track the desired trajectory at the curve C_2 , and that, with $p = -0.1$, the vehicle succeeds in tracking the complete desired trajectory.

Fig. 8. Look-below tracking. (a) $p = -0.2$. (b) $p = -0.1$.Fig. 9. Look-behind tracking. (a) $p = -0.2$. (b) $p = -0.1$.

VII. CONCLUSION

This paper analyzes the stable full-state tracking problem of nonholonomic wheeled mobile robots under output-tracking control laws. Tracking-error dynamics is a suitable means to develop the relationship between the output-tracking stability and the full-state tracking stability. It is shown that the internal dynamics and zero dynamics play a critical role of the full-state tracking stability of such mobile robots. Sufficient conditions for the stable full-state tracking offer a general approach for analysis using linear approximations. The detailed investigation of a car-like mobile robot leads to sufficient conditions for stable tracking. Numerical searching results also help further stability analysis and offer insightful observations on the selection of output functions and controller designs.

APPENDIX LEMMAS

Lemma 2 [19]: Consider the system

$$\dot{y} = g(y) \quad (74)$$

$$\dot{z} = q(y, z, t). \quad (75)$$

Suppose that

- 1) $(y, z) = (0, 0)$ is an equilibrium of (74) and (75), and the function $q(y, z, t)$ is locally Lipschitzian in (y, z) , uniformly with respect to t , i.e., there exists L (independent of t) such that

$$\|q(y', z', t) - q(y'', z'', t)\| < L(\|z' - z''\| + \|y' - y''\|)$$

for all z', z'' in a neighborhood of $z = 0$, all y', y'' in a neighborhood of $y = 0$, all $t \geq 0$;

- 2) equilibrium $z = 0$ of $\dot{z} = q(z, 0, t)$ is uniformly asymptotically stable;
- 3) equilibrium $y = 0$ of (74) is stable.

Then, the equilibrium $(y, z) = (0, 0)$ of (74) and (75) is uniformly stable.

For nonautonomous systems, Lemma 3 is a Lyapunov's linearization based results for stability analysis.

Lemma 3 [20]: Suppose that $x = 0$ is an equilibrium of the nonautonomous system

$$\dot{x} = f(x, t). \quad (76)$$

Then, for any fixed time t (i.e., regarding t as a parameter), a Taylor expansion of function f leads to

$$f(x, t) = A(t)x + f_{h.o.t.}(x, t) \quad (77)$$

where

$$A(t) = \left. \left(\frac{\partial f}{\partial x} \right) \right|_{x=0}. \quad (78)$$

Suppose that condition

$$\limsup_{\|x\| \rightarrow 0} \frac{\|f_{h.o.t.}(x, t)\|}{\|x\|} = 0 \quad \forall t \geq 0 \quad (79)$$

is satisfied. If the linearized system

$$\dot{x} = A(t)x \quad (80)$$

is uniformly asymptotically stable, the equilibrium 0 of the nonautonomous system (76) is also uniformly asymptotically stable. The linear time-varying system (80) is said to be the linear approximation of the nonlinear nonautonomous system (76) if the uniform convergence condition (79) is satisfied.

Instability of a nonautonomous system can be determined using its Taylor expansion for some cases such as the following Lemma.

Lemma 4 [20]: If the Jacobian matrix $A(t)$ defined in (78) of nonautonomous system (76) is a constant matrix A_0 , and if (79) is satisfied, then the instability of the linearized system implies that of the original nonautonomous nonlinear system, i.e., (76) is unstable if one or more of the eigenvalues of A_0 has a positive real part.

It is also known that eigenvalues all have negative real parts cannot guarantee a linear time-varying system to be stable. Nevertheless, as for slowly time-varying systems, we have following lemma.

Lemma 5 [21]: Consider the system

$$\dot{x} = A(t, \beta(t))x \quad (81)$$

with $A(t, \beta(t))$ being Lipschitz continuous in both t and $\beta(t)$ and uniformly bounded on R_+ ; and β is a vector of uniformly bounded, Lipschitz continuous time-varying parameters [i.e., $\beta(t) \in \mathcal{M}, \forall t \in R_+$, where \mathcal{M} is a bounded set]. Suppose that for every frozen $\bar{\beta} \in \mathcal{M}$ the system

$$\dot{x} = A(t, \bar{\beta})x \quad (82)$$

is exponentially stable, uniformly in $\bar{\beta}$. Further, suppose that there exist constants $\mu, c \geq 0$ such that condition

$$\int_{t_0}^{t_0+T} \|\dot{\beta}(t)\| dt \leq c + \mu T, \quad \forall T \geq 0, \forall t_0 \geq 0 \quad (83)$$

is satisfied. Then, (81) is uniformly exponentially stable.

REFERENCES

- [1] R. W. Brockett, "Asymptotic stability and feedback stabilization," in *Differential Geometric Control Theory*, R. W. Brockett, R. S. Millmann, and H. J. Sussmann, Eds. Berlin, Germany: Birkhauser, 1983, pp. 181–191.
- [2] J. Zabczyk, "Some comments on stabilizability," *Int. J. App. Math. Optim.*, vol. 19, pp. 1–9, 1989.
- [3] C. C. de Wit and O. J. Sørđalen, "Exponential stabilization of mobile robots with nonholonomic constraints," *IEEE Trans. Automat. Contr.*, vol. 37, pp. 1791–1797, Nov. 1992.
- [4] A. Astolfi, "Discontinuous control of nonholonomic systems," *Syst. Contr. Lett.*, vol. 27, pp. 37–45, 1996.
- [5] J.-B. Pomet, "Explicit design of time-varying stabilizing control laws for a class of controllable systems without drift," *Syst. Contr. Lett.*, vol. 18, pp. 147–158, 1992.
- [6] C. Samson, "Control of chained systems. Application to path following and time-varying point stabilization of mobile robots," *IEEE Trans. Automat. Contr.*, vol. 40, pp. 64–70, Jan. 1995.
- [7] O. J. Sørđalen and O. Egeland, "Exponential stabilization of nonholonomic chained systems," *IEEE Trans. Automat. Contr.*, vol. 40, pp. 35–49, Jan. 1995.
- [8] R. T. M'Closkey and R. M. Murray, "Exponential stabilization of driftless nonlinear control systems using homogeneous feedback," *IEEE Trans. Automat. Contr.*, vol. 42, pp. 614–628, May 1997.
- [9] N. Sarkar, X. P. Yun, and V. Kumar, "Control of mechanical systems with rolling constraints: Applications to dynamic control of mobile robots," *Int. J. Robot. Res.*, vol. 13, pp. 55–69, 1994.
- [10] C. Y. Su and Y. Stepanenko, "Robust motion/force control of mechanical systems with classical nonholonomic constraints," *IEEE Trans. Automat. Contr.*, vol. 39, pp. 609–614, Mar. 1994.

- [11] G. Campion, G. Bastin, and B. d'Andréa Novel, "Structural properties and classification of kinematic and dynamic models of wheeled mobile robots," *IEEE Trans. Robot. Automat.*, vol. 12, pp. 47–62, Feb. 1996.
- [12] S. V. Gusev, I. A. Makarov, I. E. Paromtchik, and C. Laugier, "Adaptive motion control of nonholonomic vehicle," in *Proc. 1998 Int. Conf. Robotics and Automation*, Leuven, Belgium, May 1998, pp. 3285–3290.
- [13] J. M. Yang and J. H. Kim, "Sliding mode control for trajectory tracking of nonholonomic wheeled mobile robots," *IEEE Trans. Robot. Automat.*, vol. 15, pp. 578–587, June 1999.
- [14] Y. Kanayama, Y. Kimura, F. Miyazaki, and T. Noguchi, "A stable tracking control method for an autonomous mobile robot," in *Proc. 1990 Int. Conf. Robotics and Automation*, 1990, pp. 384–389.
- [15] G. C. Walsh, D. Tilbury, S. Sastry, R. Murray, and J. P. Laumond, "Stabilization of trajectory for systems with nonholonomic constraints," *IEEE Trans. Automat. Contr.*, vol. 39, pp. 216–222, Jan. 1994.
- [16] Z. P. Jiang and H. Nijmeijer, "A recursive technique for tracking control of nonholonomic systems in chained form," *IEEE Trans. Automat. Contr.*, vol. 44, pp. 265–279, Feb. 1999.
- [17] X. P. Yun and Y. Yamamoto, "Stability analysis of the internal dynamics of a wheeled mobile robot," *J. Robot. Syst.*, vol. 14, no. 10, pp. 697–709, 1997.
- [18] B. d'Andréa Novel, G. Campion, and G. Bastin, "Control of nonholonomic wheeled mobile robots by state feedback linearization," *Int. J. Robot. Res.*, vol. 14, pp. 543–559, 1995.
- [19] A. Isidori, *Nonlinear Control System*, 2nd ed. Berlin, Germany: Springer-Verlag, 1989.
- [20] J.-J. E. Slotine and W. P. Li, *Applied Nonlinear Control*. Englewood Cliffs, NJ: Prentice-Hall, 1991.
- [21] K. S. Tsakalis and P. A. Ioannou, *Linear Time-Varying Systems Control and Adaptation*. Englewood Cliffs, NJ: Prentice-Hall, 1993.



Danwei Wang received the B.E. degree from the South China University of Technology, GuangZhou, China in 1982, and the M.S.E. and Ph.D. degrees from the University of Michigan, Ann Arbor, in 1985 and 1989, respectively.

Since 1989, he has been with the School of Electrical and Electronic Engineering, Nanyang Technological University, Singapore, where he is currently an Associate Professor and Deputy Director of the Robotics Research Center. His research interests include robotics, control theory and applications. He has published more than 100 technical articles in the areas of iterative learning control, robust control and adaptive control systems, as well as manipulator/mobile robot dynamics, path planning, and control.

He has served as General Chairman, Technical Chairman and in various other positions in international conferences, such as International Conference on Control, Automation, Robotics and Vision (CARCVs) and Asian Conference on Computer Vision (ACCV). He is an Associate Editor of Conference Editorial Board, IEEE Control Systems Society and an active member of IEEE Singapore Robotics and Automation Chapter. He was a recipient of the Alexander von Humboldt fellowship, Germany. (Personal home page: <http://www.ntu.edu.sg/home/edwwang>.)

Guangyan Xu, photograph and biography not available at the time of publication.